Journal of Molecular Liquids 410 (2024) 125675

Contents lists available at ScienceDirect

Journal of Molecular Liquids

journal homepage: www.elsevier.com/locate/molliq

Supramolecular engineering of micellar systems: Precision control on self-assembly, polarity, and charge for enhanced nanocarrier design

Borja Gómez-González [a], Nuno Basílio [b], Belén Vaz [c,d], Karen V. Góñez [e], Moisés Pérez-Lorenzo [c,d,*], Luis García-Río [a,*]

[a] Department of Physical Chemistry, Universidade de Santiago de Compostela, Santiago de Compostela 15782, Spain
[b] Laboratório Associado para a Química Verde (LAQV), Rede de Química e Tecnologia (REQUIMTE), Departamento de Química, Faculdade de Ciências e Tecnologia, Universidade NOVA de Lisboa, Caparica 2829-516, Portugal
[c] CINBIO, Universidade de Vigo, Vigo 36310, Spain
[d] Galicia Sur Health Research Institute, Vigo 36310, Spain
[e] Centro de Investigación Mestrelab (CIM), Av. Barcelona 7, Santiago de Compostela 15706, Spain

ARTICLE INFO

Keywords:
Self-assembly
Supramolecular micelle
Macrocyclic receptor
Nanocarrier design
Environment-sensitive probe

ABSTRACT

In the quest for enhanced drug delivery systems, the combination of supramolecular receptors and surfactants represents a promising step toward developing innovative and highly efficient nanocarriers. This research highlights the paramount advantages of synergizing these elements, focusing on the manipulation of the self-assembly, charge, and polarity of the hybrid nanostructures resulting from merging these building blocks. In this vein, this work reveals that the integration of hexamethylated p-sulfonatocalix[6]arene (SC6A) and dodecyltrimethylammonium bromide (DTAB) offers significant advantages over those colloidal nanostructures stemming from the use of surfactant alone. These include the ability to stimulate early self-assembly, thereby facilitating the formation of stable nanocarriers, even in high-dilution scenarios. Additionally, the electrostatic balance established within the macrocycle-surfactant host–guest complexes can be harnessed to finely adjust the charge of the hydrophilic micellar corona. This holds great promise for modulating the bio-interaction capabilities of nanocarriers. Furthermore, the inclusion of the macrocycle in the colloidal structure induces significant alterations in the arrangement of low-molecular-weight surfactants. This leads to a significant transformation in the hydrophobic properties of the micellar core, which can be exploited to tailor this microenvironment to match the lipophilicity of specific drugs. In this regard, our findings reveal that while conventional DTAB micelles generally replicate the polarity of a solvent with a dielectric constant of 37.7, engineered SC6A-DTAB aggregates demonstrate a capability to reach a polarity akin to a solvent with dielectric constant of 17.5. This spectrum of hydrophobicities within the micellar core represents a significant advancement and opens up new possibilities for drug delivery applications.

1. Introduction

Over the years, micelles have garnered significant attention in the biomedical field due to their unique properties and versatility [1–5]. These nanoscale carriers hold the potential to transform drug delivery as they can address crucial challenges in modern medicine such as enhancing the efficacy and precision of treatments, minimizing adverse side effects, and optimizing therapeutic outcomes [6–10]. At this point, it is important to note that the distinctive characteristic of micelles lies in their spontaneous self-assembly in aqueous solution, driven by the amphiphilic nature of their constituent molecules [11]. On one hand, their hydrophobic cores allow for the efficient encapsulation of hydrophobic drugs, enhancing the solubility, stability, and bioavailability of the active ingredient [12,13]. On the other hand, their hydrophilic corona enables micelles to circulate effectively in the bloodstream, interact with biological molecules, and target specific cells or tissues, thereby minimizing off-target effects and optimizing drug delivery efficiency [14,15]. In this regard, it is worth highlighting that micelles can be endowed with diverse functionalities, enabling responsiveness to a wide array of stimuli (either of endogenous or exogenous origin)

* Corresponding authors at: CINBIO, Universidade de Vigo, Vigo 36310, Spain (M. Pérez-Lorenzo), Department of Physical Chemistry, Universidade de Santiago de Compostela, Santiago de Compostela 15782, Spain (L. García-Río).
E-mail addresses: moisespl@uvigo.es (M. Pérez-Lorenzo), luis.garcia@usc.es (L. García-Río).

https://doi.org/10.1016/j.molliq.2024.125675
Received 22 April 2024; Received in revised form 27 July 2024; Accepted 31 July 2024
Available online 2 August 2024

[16,17]. This versatility significantly enhances their targeting precision. Along these lines, when designing these colloidal structures in biomedical research, polymers have usually been the surfactants of choice, somewhat overshadowing traditional low-molecular-weight (LMW) surfactants (typically below 500 g/mol) [18–21]. This is largely due to the rich nature of polymer chemistry, which allows for precise control over micelle size, drug loading, and release kinetics [22]. Another advantage of polymeric micelles over those derived from LMW surfactants is their lower critical micelle concentration (CMC), and as a result, their higher stability and prolonged transit times in biological environments [23]. This enhanced consistency ensures a longer-lasting presence in the vascular system, facilitating sustained drug delivery and increasing the likelihood of therapeutic success [24]. However, despite all these strengths, polymer synthesis can be complex, and issues related to regulatory approval, batch-to-batch variability and scalability may easily arise [25–27].

Unlike their polymeric counterparts, synthetic and natural LMW surfactants stand out for their ease of synthesis and characterization, making them appealing candidates for drug delivery applications as they can address some of the previously described problems [28–31]. However, these surface-active agents still face a series of significant limitations. As indicated above, one of these drawbacks is their inherently high CMC compared to amphiphilic polymers, which results in premature disassembly in physiological settings. This issue reduces their circulation time in vivo and raises concerns about their stability [32]. Furthermore, low-molecular-weight surfactant-based carriers may not entrap hydrophobic drugs as effectively as the typically used amphiphilic block polymers (generally in the range of kDa), such as PEO-b-poly(aminoacid)s, PEO-b-poly(ester)s, and Pluronic® [33]. This limitation could potentially restrict the therapeutic efficacy of the surfactant-based carriers [34]. Additionally, it is important to consider aspects related to their electrostatics, as this parameter may have a major impact on potential interactions within biological systems, thereby playing a crucial role in the performance of micelles as effective therapeutic carriers [35]. With all of this in mind, it becomes evident that modulating the self-aggregation behavior of LMW surfactants, as well as the hydrophobicity and charge of the resulting colloidal structures, is essential for optimizing their stability, encapsulation efficiency, as well as targeting abilities and thus, their overall efficacy in drug delivery applications within the complex biological milieu.

To address these challenges, the present study builds upon the advancements in supramolecular amphiphiles,[36] harnessing the synergistic capabilities of macrocyclic receptors and low-molecular-weight (LMW) surfactants arranged in host–guest configurations [37]. This

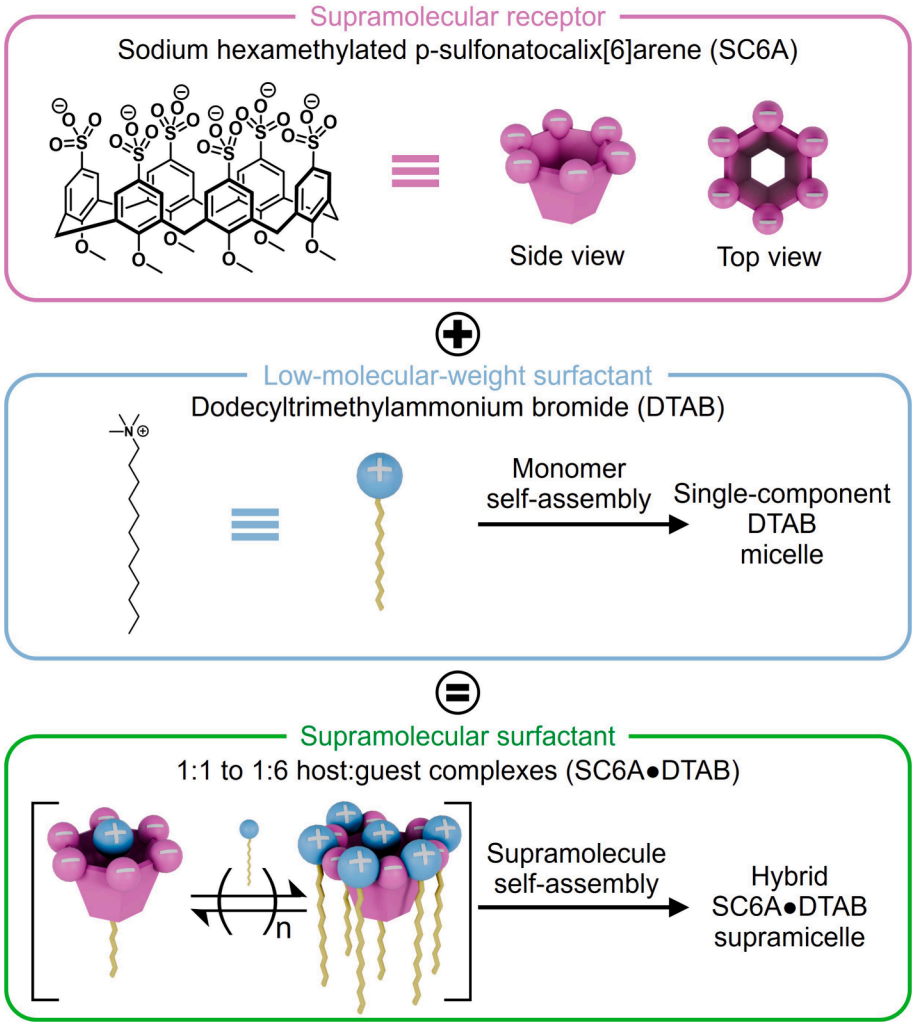

Scheme 1. Illustration portraying the fundamental building blocks utilized in the formation of the supramolecular surfactants for generating the hybrid micelles elucidated in this study, along with a schematic representation of the host–guest complexes that self-assemble to give rise to the supramolecular nanocarriers reported herein. In this case, the initial formation of a 1:1 inclusion complex between SC6A and DTAB is suggested, followed by the progressive incorporation of additional DTAB molecules through the formation of an external complex. This model is based on the significant steric hindrance that additional DTAB molecules would encounter if attempting to enter the internal cavity of a calixarene where one DTAB molecule is already accommodated.

strategy is rooted in the demonstrated proficiency of such architectures to regulate the formation of micelles and fine-tune the physicochemical attributes of these aggregates [38]. Along these lines, this approach not only tackles the limitations of traditional surfactant systems but also opens new avenues for the precise design of micellar nanocarriers. In this vein, this supramolecular strategy is projected to significantly influence key structural parameters of these assemblies, such as CMC, polarity, and charge, thereby enhancing their efficacy as drug transporters. With this aim, a combination of multianionic receptor sodium hexamethylated p-sulfonatocalix[6]arene (SC6A) as a host and cationic surfactant dodecyltrimethylammonium bromide (DTAB) as a guest is employed as a model system (Scheme 1). The rationale behind selecting anionic calixarenes for this study lies in their significant potential for biomedical applications [39]. Specifically, amphiphilic calixarenes, which have the ability to self-assemble and solubilize various active pharmaceutical ingredients, are of particular interest [40]. By exploiting the unique binding properties of SC6A, it is anticipated that precise control over the resulting DTAB-based micelles can be attained. In this context, it is expected that this level of control can be used to tune CMC, thereby offering the potential to reinforce the stability of micellar structures under high-dilution regimes, such as those commonly found in biological environments. Moreover, the incorporation of the macrocycle into the colloidal structure is predicted to induce significant modifications in the packing of the LMW surfactants, leading to a substantial alteration in the hydrophobic nature of the micellar core and thus, improving the encapsulation efficiency of lipophilic drugs. Furthermore, it is foreseeable that the electrostatic equilibrium established within the calixarene-surfactant host–guest complexes may be employed to adjust the charge of the hydrophilic micellar crown, thus holding substantial promise for enhancing the potential bio-interactions of the nanocarrier. Ultimately, this supramolecular strategy has the potential to pave the way for the development of LMW surfactant-based micelles whose structural parameters may be easily tailored to fulfill different needs in terms of biomedical applications.

2. Results and discussion

As a preliminary step, the assessment of the self-aggregation behavior exhibited by DTAB is conducted. To achieve this, Prodan (N, N-dimethyl-6-propionyl-2-naphthylamine) is employed as a solvatochromic fluorescent probe due to its exceptional optical response to changes in local polarity as well as hydrogen bonding interactions within the surrounding microenvironment [41,42]. As known, as surfactant molecules self-aggregate, they create microdomains with varying polarities. Prodan, owing to its high sensitivity to such changes, undergoes modifications in its emission properties as a result. Thus, by monitoring changes in its emission wavelength and intensity, valuable insights into the dynamics of the surfactant self-aggregation can be gained. Notably, one of the key advantages of Prodan over other solvatochromic probes lies in its lack of permanent charge within its molecular structure. This specific attribute mitigates the potential for interference between this dye and the constituent components of the micelle. This renders this probe an ideal candidate for conducting these studies as its presence within the aggregate neither introduces additional electrostatic effects nor disrupts the micellar assembly.

Fig. 1a depicts the fluorescence spectra of Prodan at increasing concentrations of DTAB. As observed, there is a dual alteration in the emission spectrum of this probe as the surfactant concentration rises. This concomitant variation involves a blueshift in the Prodan's wavelength of maximum emission (λ_{max}) and a significant increase in fluorescence intensity. This behavior is associated with the incorporation of the solvatochromic probe into a microdomain with lower polarity than that provided by the solvent. These trends are more clearly illustrated in Fig. 1b. At low surfactant concentrations, λ_{max} closely matches that of pure water, located around 522 nm. Then, upon reaching a DTAB concentration of $\sim 10^{-2}$ M, there is a sharp decrease in λ_{max} due to the

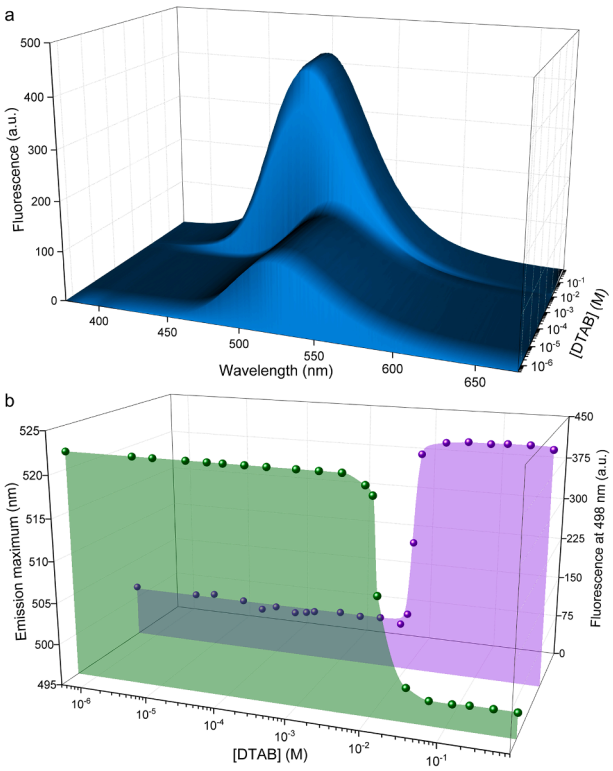

Fig. 1. (a) Fluorescence spectra of Prodan (1.0×10^{-6} M) in the presence of increasing concentrations of DTAB (ranging from 5.0×10^{-7} M to 0.8 M) in aqueous solution. λ_{exc} = 343 nm. T=25.0 °C; and (b) Influence of DTAB concentration on the wavelength of maximum emission (green) and the fluorescence intensity at 498 nm (purple) (data extracted from a).

incorporation of the hydrophobic probe into the formed micellar aggregates. This concentration corresponds to the CMC of DTAB and closely aligns with values reported in the literature using alternative techniques [43]. Following this decline, Prodan's emission maximum stabilizes at 498 nm, indicating an equilibrium where the fluorescent probe is clearly shifted toward the micellar environment. Notably, the λ_{max} value reached at high DTAB concentrations offers insights into the attained level of polarity. In this regard, this wavelength serves as a key metric for estimating the Reichardt's $E_T(30)$ parameter, which quantifies the polarity of a microenvironment based on the position of the absorption or emission band of a given solvatochromic probe [44]. Thus, a higher $E_T(30)$ value indicates a more polar microenvironment, whereas a lower value signifies a less polar one. In this case, 498 nm suggests that the nature of the micellar core resembles that of a glycol solution [45]. This lower polarity, in comparison to water, indicates the potential efficacy of these assemblies as carriers for certain lipophilic drugs. As depicted in Fig. 1b, the conclusions drawn from the evolution of the fluorescence emission maximum with DTAB concentration are further supported by the simultaneous change observed in the fluorescence intensity of the probe, which markedly increases upon reaching the CMC. This phenomenon is attributed to the progressive accumulation of Prodan within the formed assemblies, resulting in a substantial reduction in the nonradiative deexcitation pathways for its excited state [46].

Having reached this point, it is imperative to highlight the good agreement between the results obtained using Prodan and other alternative techniques. This solid alignment serves to validate the use of Prodan as a solvatochromic fluorophore for investigating self-assembly phenomena in ionic surfactants, thereby endorsing its application in the study of DTAB in the presence of supramolecular receptors. In this context, Fig. 2a illustrates the changes in Prodan's emission spectrum as a function of DTAB concentration in the presence of a fixed amount of

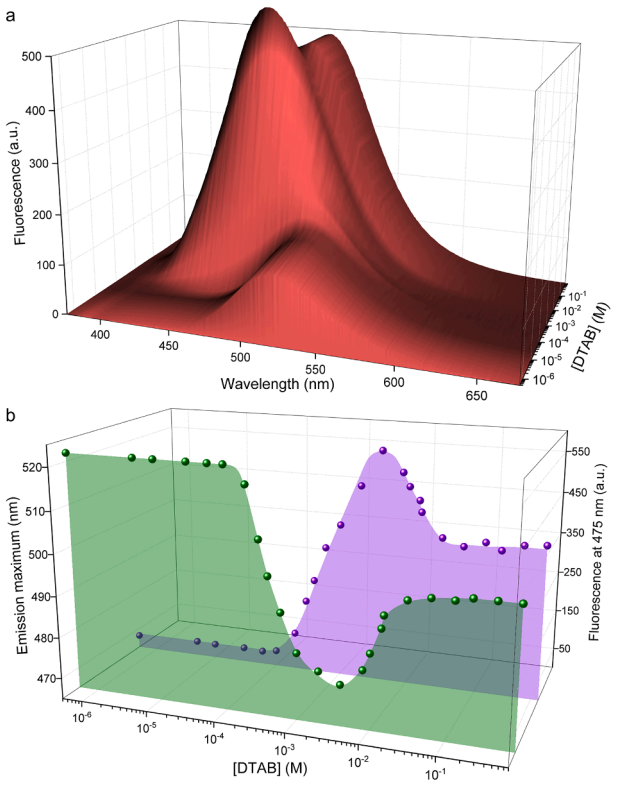

Fig. 2. (a) Fluorescence spectra of Prodan (1.0×10^{-6} M) in the presence of increasing concentrations of DTAB (ranging from 5.0×10^{-7} M to 0.8 M) in aqueous solution in the presence of SC6A (5.0×10^{-4} M). λ_{exc} = 343 nm. T=25.0 °C; and (b) Influence of DTAB concentration on the wavelength of maximum emission (green) and the fluorescence intensity at 475 nm (purple) (data extracted from a).

calixarene SC6A. In an initial analysis, and mirroring the results shown in Fig. 1, a blueshift in the peak of Prodan's fluorescence emission spectrum is observed. This spectral shift is concomitant with a substantial increase in the intensity of its spectral bands. These observations are consistent with the incorporation of this fluorescent probe into the micellar aggregates formed upon reaching the necessary critical concentration of DTAB. In this scenario, the formation of an inclusion complex between Prodan and SC6A has been ruled out (Sections 2 and 3 in the SI), indicating that the probe is located within the hydrophobic micellar core. Nevertheless, a more detailed examination of these results is necessary.

Fig. 2b provides a clearer representation of the variation in Prodan's wavelength of emission maximum as a function of DTAB concentration in the presence of SC6A. Herein, it becomes evident that at low surfactant concentrations, λ_{max} (522 nm) precisely matches the value recorded for the probe in aqueous medium in the absence of DTAB. This correspondence suggests that within this concentration range, self-assembly phenomena are absent, thus indicating that the medium exhibits a homogeneous nature at a microscopic level. Upon reaching a DTAB concentration of $\sim10^{-4}$ M, λ_{max} initiates a noticeable blueshift, indicating the formation of micellar aggregates and the incorporation of the solvatochromic probe into these colloidal structures. It is worth noting that the CMC of the hybrid system is substantially lower than that observed in pure DTAB solutions ($\sim10^{-2}$ M), which is consistent with previous findings [47]. This enhanced propensity for micellization arises from the increased tendency of SC6A:DTAB complexes to self-aggregate, signifying greater stability of the supramolecular micelles compared to those derived from surfactant alone, especially at high dilution regimes. In this context, the self-aggregation of these host:guest structures has been previously demonstrated through dynamic light scattering measurements, which show that SC6A:DTAB micelles are larger compared to micelles solely based on DTAB [48]. This greater inclination toward micellization can be attributed to the interaction of DTAB with SC6A, which effectively mitigates the electrostatic repulsion between the surfactant headgroups. As a result, the formation of the hybrid architecture becomes enthalpically more favorable compared to its single-component counterpart [49,50]. Consequently, in terms of applicability, it is evident that these hybrid colloidal structures hold significant potential as nanocarriers in comparison to conventional micelles. Furthermore, it is crucial to highlight that within this concentration range, where SC6A is in excess relative to the surfactant, the resulting micelles carry a net negative surface charge. This is ascribed to the charge imbalance within the host–guest complexes that comprise the colloidal aggregate, with the calixarene contributing six negative charges in contrast to the single positive charge provided by the surfactant [51]. This imbalance is a pivotal factor to consider, given the paramount role of the charge of the hydrophilic corona in the performance of nanocarriers in terms of circulation times and bio-interactions [52].

The steep decline initiated after surpassing the CMC continues until reaching a DTAB concentration of approximately 3.0×10^{-3} M at which a minimum for λ_{max} is observed. It is worth underlining that such a minimum is achieved when the surfactant-to-calixarene concentration ratio stands at 6:1. As depicted in Scheme 2, it is precisely in this concentration ratio that an efficient and orderly packing of the hydrophobic DTAB chains induced by the presence of calixarene occurs. This results in the formation of micellar cores with a high degree of compactness and hence highly hydrophobic character [53]. This efficient arrangement of the alkyl chains ultimately leads to a blueshift of Prodan to 475 nm. At this point, it should be noted that the solvatochromic shift in micelles derived from DTAB alone only extends to 498 nm, underscoring that supramolecular micelles provide a less polar environment than purely surfactant-based carriers, and hence pinpointing that these hybrid systems may potentially serve as more efficient carriers for highly lipophilic active ingredients. Thus, if the polarity of the micellar core derived from the use of DTAB resembles that of a glycol solution, the interior of the supramolecular micelles can be likened to a solution where 1-amino-2-propanol is employed as the solvent [45]. In this context, it is also interesting to note that the difference in polarity between conventional and supramolecular micelles is of a magnitude akin to that observed between water and regular micelles. This provides a clear indication of the significant influence exerted by macrocyclic receptors on the structural parameters of these self-assembled nanostructures. It is important to highlight that the established DTAB:SC6A ratio of 6:1 at the minimum of the curve in Fig. 2b is intrinsically tied to the equilibrium of charges within the supramolecular surfactants, and consequently, to the overall charge of the resulting micellar system. Thus, reaching the highest level of DTAB monomer supramolecular packing coincides with the point where the charges of DTAB and SC6A offset each other, resulting in a micellar structure with a net zero charge (Scheme 2 and Section 6 in the SI). This indicates a transition of the micelles to a state of neutrality, carrying significant implications for their potential function as nanocarriers.

Further dissecting Fig. 2b, once the minimum of the curve is surpassed, there is an evident increase indicating a redshift in the wavelength of the Prodan's emission peak. This rise persists until a λ_{max} coincident with that obtained with conventional micelles (Fig. 1b) is reached. The observed trend herein can be explained by the progressive increase in DTAB concentration (Section 5 in the SI). Once the point of electrostatic charge neutralization is achieved, adding further surfactant induces the formation of positively charged micelles due to the incorporation of extra DTAB molecules into the aggregates (Scheme 2, and Sections 3–5 in the SI), as demonstrated by the evolution of the surface charge of the micelles (Section 6 in the SI). This compaction is followed by a gradual increase in the concentration of free DTAB monomers (Section 5 in the SI). Once their CMC is reached, pure surfactant-based

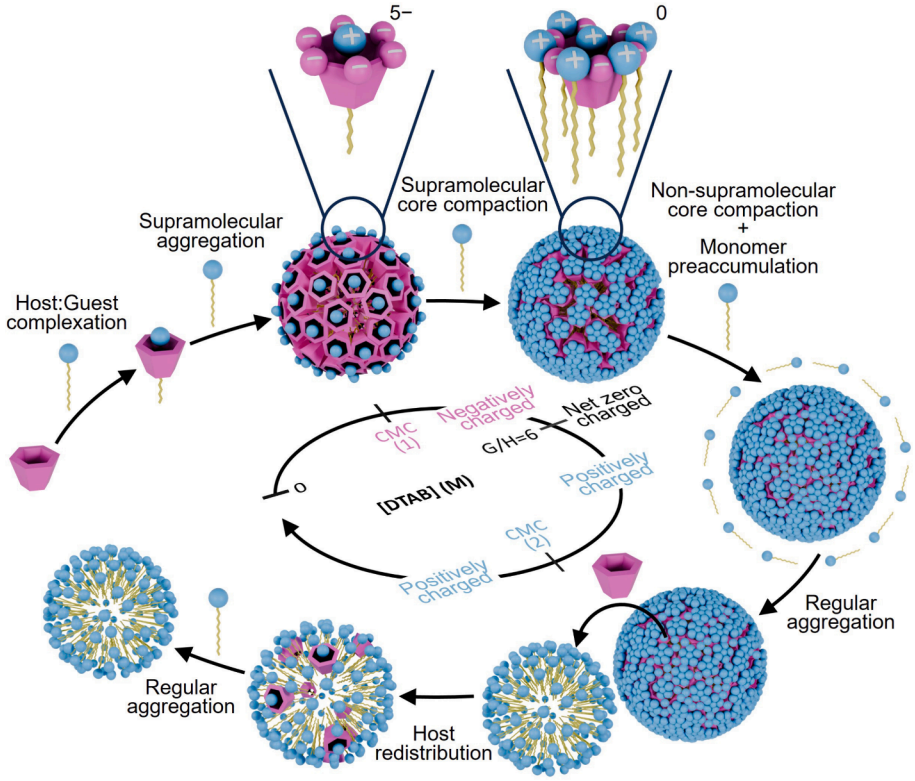

Scheme 2. Illustration providing a visual representation of the diverse events of host–guest complexation and amphiphilic aggregation occurring in response to increasing surfactant concentration in aqueous solution. Herein, the dynamic evolution of these phenomena is depicted, offering insights into the changing properties of the resulting nanocarriers in terms of assembly, hydrophobicity, and surface charge.

micelles are once again obtained [47]. Evidently, since conventional and supramolecular micelles cannot coexist in solution, an instantaneous redistribution of SC6A occurs between both types of aggregates to maintain thermodynamic equilibrium (Scheme 2). This behavior leads to the formation of mixed structures with a lower content of macrocycle per aggregate, or in other words, with a surfactant-to-calixarene ratio exceeding the 6:1 value. In this context, this phenomenon has a dual impact on the properties of the resulting micelles. Firstly, it results in a decreased compactness of the hydrophobic core. This increases the polarity of the microenvironment to which the solvatochromic probe is exposed, consequently leading to a redshift in its fluorescence emission spectrum. As a result, the optical behavior of Prodan in the presence of SC6A at high DTAB concentrations corresponds to what has been previously illustrated in Fig. 1 for pure micelles. Secondly, surpassing the 6:1 ratio induces a change in the carrier surface charge, shifting from a neutral to a positive charge, which bears significant implications in terms of potential bio-interactions.

The conclusions drawn from the analysis of the solvatochromic shift of Prodan are again further supported by the examination of the fluorescence intensity of this probe. As depicted in Fig. 2b, the emission intensity of this dye at 475 nm initially corresponds to the value obtained in pure water. Once the CMC is surpassed, fluorescence progressively increases due to the gradual accumulation of the probe inside the emergent supramolecular micelles. This intensity increase continues until it reaches a maximum, which corresponds to the point of charge neutralization between DTAB and SC6A, at which the hybrid micelles with the lowest polarity are formed. Beyond this value, a further increase in DTAB concentration leads to a decrease in fluorescence intensity as the environment probed by Prodan transitions to the micellar structures featuring a progressively less densely packed core and, consequently, higher polarity. This decrease continues until a DTAB concentration of $\sim 10^{-2}$ M is reached. At this stage, the intensity value aligns with that observed in the case of micelles derived from DTAB alone. This is an expected outcome, considering that the supramolecular micelles in this concentration range exhibit a low calixarene content, making them resemble those micelles based exclusively on DTAB (Scheme 2). Indeed, at exceptionally high surfactant-to-calixarene ratios, micelle formation inevitably occurs without the accommodation of calixarene molecules on their surface, given the substantial excess concentration of surfactant compared to that of macrocycle.

At this stage, it is crucial to highlight the inherent potential of the system at hand. In this regard, this type of hybrid colloidal structures enables fine-tuning the charge of the hydrophilic corona of the carrier through a straightforward manipulation of the surfactant-to-macrocycle ratio. This is of paramount importance due to the role of the micellar surface charge in circulation and interactions with serum components, cell membranes, and intracellular organelles. Along these lines, it has been reported that neutral or negatively charged micelles exhibit longer circulation times compared to positively charged micelles [54]. This is because the latter are more susceptible to sequestration by macrophages constituting the mononuclear phagocyte system. Conversely, positively charged micelles demonstrate an increased likelihood of nonspecific uptake by most cells. Furthermore, nanocarriers exhibiting a positive charge are known to promote endosomal release, thereby avoiding the degradative effects of the endosomal compartment on the cargo [55]. Considering these trends, it becomes clear that a neutral or negative micelle surface charge is preferable upon administration, with a transition to a positive charge upon reaching the target site proving highly advantageous. This is where supramolecular micelles can serve as an interesting alternative to other charge-reversing approaches described in the literature, given their potential to alter their charge based on the surfactant-to-macrocycle concentration ratio [56,57]. It is also worth noting that this change in surface charge is actually inherent to the change in the density of the micellar core. This aspect could be harnessed to induce the release of highly lipophilic cargoes contained within this nanocarrier. In this regard, it is essential to remember that

the transition to a positively charged hydrophilic corona is brought about by the formation of hybrid micelles with a lower macrocycle content, resulting in reduced compactness of the arrangement of the DTAB hydrocarbon chains. This decompaction leads to increased core polarity and, consequently, may be potentially exploited to induce the release of highly lipophilic drugs encapsulated within.

At this point, it is essential to examine how alterations in macrocycle concentration impact the self-aggregation phenomena within supramolecular micelles. Fig. 3a provides insight into the effect of calixarene concentration on the formation of these colloidal aggregates. While, in broad terms, the observed trends align with those in Fig. 2, there are several aspects deserving of highlight. First, it is noticeable that in all cases the blueshift of Prodan begins upon reaching a DTAB concentration of $\sim 10^{-4}$ M. This observation implies that the CMC remains constant regardless of the SC6A concentration, confirming the significant capacity of these supramolecular receptors to foster early micellization phenomena in LMW surfactants and consequently, promoting the creation of stable nanocarriers even in highly diluted regimes. However, the observed blueshift reveals distinct patterns. At low concentrations of calixarene (0–4×10^{-5} M), a gradual hypsochromic shift of the fluorophore is evident. Initially, at a DTAB concentration of $\sim 10^{-4}$ M, the formation of supramolecular micelles triggers the initial blueshift. This phase is followed by a plateau (in the millimolar concentration range) where no new aggregates form, thus resulting in no alteration in the fluorescence emission maximum. Upon reaching a DTAB concentration of $\sim 10^{-2}$ M, an increasing number of new micelles form, facilitating the partitioning of Prodan into these hydrophobic cores, leading to a second hypsochromic shift, reaching 498 nm. On the other hand, at high concentrations of calixarene (4×10^{-5} to 1×10^{-3} M), the results obtained are analogous to those previously shown in Fig. 2. At this stage, it is crucial to note the evolution of the point of electrostatic charge neutralization. This threshold, easily identifiable due to its alignment with the minima in the various curves depicted in Fig. 3a, is reached, as

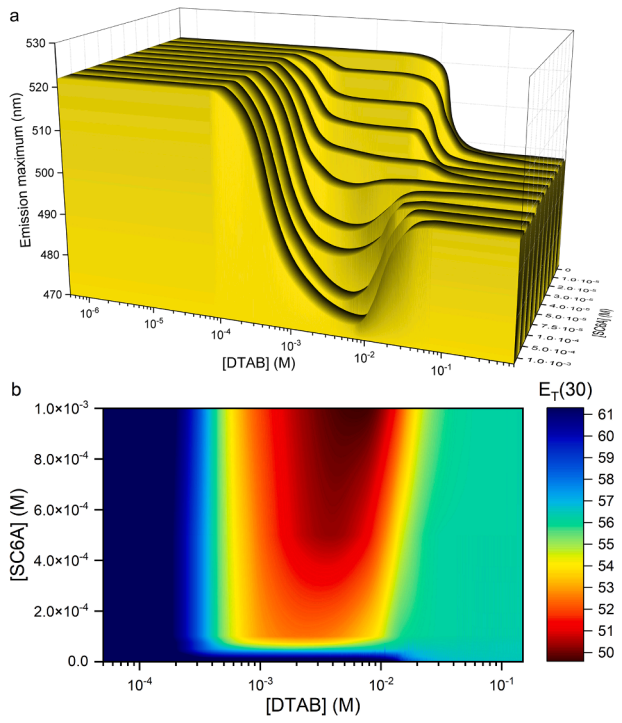

Fig. 3. (a) Influence of DTAB concentration on the Prodan's wavelength of maximum emission (1.0×10^{-6} M) in the presence of increasing concentrations of SC6A (ranging from 0 M to 1.0×10^{-3} M). λ_{exc} = 343 nm. T=25.0 °C; and (b) Contour plot of the influence of DTAB and SC6A on the Reichardt's empirical $E_T(30)$ polarity parameter.

previously explained, when the surfactant-to-calixarene concentration ratio stands at 6:1. Naturally, this accounts for why this minimum shifts to higher DTAB concentrations as SC6A concentration increases. What is particularly interesting is to observe that as the macrocycle concentration rises, the blueshift of Prodan at this charge neutralization point becomes increasingly pronounced, eventually reaching 473 nm. In this context, the Prodan's emission maximum in the supramolecular micelles may shift up to 50 nm. Certainly, this trend suggests that the macrocycle content plays a pivotal role in the micellar core density, and consequently, in its hydrophobicity and its ability to host highly lipophilic active compounds. This underscores the major impact of these receptors on the structural features of micelles, and as previously mentioned, the significantly lower degree of polarity of supramolecular self-assembled nanostructures compared to conventional colloids. Lastly, under high DTAB concentrations, Prodan's fluorescence spectrum consistently mirrors that of pure micelles, irrespective of the SC6A concentration. It is worth highlighting that within this concentration range, micelles solely derived from DTAB coexist with supramolecular micelles which is thermodynamically unfeasible. This leads to a swift redistribution of the macrocycle between both aggregate types to restore equilibrium. This ultimately brings about the creation of micelles with a low calixarene content, and as a result, structural characteristics that resemble those of conventional micelles. At significantly elevated surfactant-to-calixarene ratios, micelles even lack calixarene molecules on their surface, owing to the substantial surplus concentration of surfactant compared to that of macrocycle.

Once the various fluorescence emission maxima of Prodan are determined as a function of different concentrations of surfactant and macrocycle, it becomes possible to assess the polarity of the different scenarios within the Reichardt's solvent polarity scale. This can be easily achieved by determining the empirical solvent polarity parameter $E_T(30)$ (Section 7 in the SI). The results obtained are shown in Fig. 3b. As observed, at low concentrations of DTAB, the polarity perceived by the chemical probe corresponds to that of water ($E_T(30) = 63.1$) [45]. As the surfactant concentration increases, there is a clear decrease in polarity due to the formation of supramolecular micelles. This decrease is only delayed in the absence of calixarene, which logically prevents early micellization of DTAB. It is also noteworthy that, as expected, regions characterized by a lower $E_T(30)$ are those where the DTAB:SC6A concentration ratio is close to 6:1. Thus, it can be observed how, as the concentration of calixarene increases, the regions of lower polarity progressively shift towards higher surfactant concentrations, reaching polarity values equivalent to those shown by Prodan in the presence of n-butanol ($E_T(30) = 49.7$; $\varepsilon_r = 17.5$) [45]. In all cases, a progressive increase in surfactant concentration leads to the formation of pure micelles, consequently resulting in the rapid redistribution of calixarene between both types of aggregates (Scheme 2). This leads to the formation of micelles with a decreasing calixarene content, whose polarity features ultimately barely differ from the polarity of micelles constituted by DTAB alone. Consequently, when DTAB concentrations surpass $\sim 10^{-2}$ M, Prodan detects a polarity akin to that observed when immersed in glycol ($E_T(30) = 56.3$; $\varepsilon_r = 37.7$) [45]. Based on these findings, it becomes apparent that, with a view to utilizing these hybrid systems as nanocarriers for highly lipophilic active ingredients, special attention must be paid to the stoichiometry of the host–guest complexes. Thus, it is vital to maximize the loading capacity of these macrocycles to induce the formation of highly hydrophobic cores. It is also important to note that surpassing the inherent CMC of the surfactant alone results in the formation of micellar aggregates that induce macrocycle redistribution, thereby disturbing the properties of the supramolecular colloids. Furthermore, the results indicate that an increase in macrocycle concentration leads to a higher degree of hydrophobicity in the micellar cores. In this regard, the interior of these micelles appears more effectively shielded from the solvent in the presence of guest-containing multicharged calixarenes than in the presence of solely DTAB molecules. This shielding effect can be attributed to the remarkable charge

delocalization of the functional groups at the portals of the calixarene, coupled with the decreasing polarity of those portals as more guest molecules are accommodated within the macrocycle's cavity.

3. Conclusions

The results of this study underscore the enormous potential inherent in harnessing supramolecular receptors and low-molecular-weight surfactants for the development of advanced nanocarriers. The strategic fusion of these building blocks unveils a range of compelling advantages. Notably, this combination empowers the initiation of early self-assembly phenomena, ensuring the creation of stable nanocarriers, a capability typically associated with polymeric micelles. Furthermore, the incorporation of macrocycles into colloidal structures induces modifications in the arrangement of low-molecular-weight surfactants, resulting in a significant change in micellar core density and, consequently, its hydrophobic nature. This transformative effect may be employed in order to enhance encapsulation efficiency, thereby facilitating more effective nanosized drug vehicles. Moreover, by leveraging the electrostatic charge equilibrium established within macrocycle-surfactant host–guest complexes, precise control over the charge of the hydrophilic micellar corona is achieved. This ability to modulate surface charge holds immense promise for fine-tuning the nanocarrier's bio-interactions through adjustment of the surfactant-to-macrocycle concentration ratio. In conclusion, the exploration of supramolecular micelles highlights their significant potential for advancing the design of novel nanocarriers, paving the way for promising developments in biomedical research.

CRediT authorship contribution statement

Borja Gómez-González: Methodology, Investigation, Formal analysis. **Nuno Basílio:** Writing – review & editing, Writing – original draft, Funding acquisition, Formal analysis. **Belén Vaz:** Writing – review & editing, Writing – original draft, Funding acquisition, Formal analysis. **Karen V. Góñez:** Writing – review & editing, Funding acquisition, Formal analysis. **Moisés Pérez-Lorenzo:** Writing – review & editing, Writing – original draft, Funding acquisition, Formal analysis, Conceptualization. **Luis García-Río:** Writing – review & editing, Writing – original draft, Funding acquisition, Formal analysis, Conceptualization.

Declaration of competing interest

The authors declare that they have no known competing financial interests or personal relationships that could have appeared to influence the work reported in this paper.

Data availability

All data are included in the article and the Supplementary Material.

Acknowledgments

This work was funded by Ministerio de Ciencia e Innovación (PID2020-113704RB-I00), Xunta de Galicia (Centro Singular de Investigación de Galicia-Accreditation 2019-2022 ED431G 2019/06, ED431C 2022/24, ED431C 2021/45, and 001_IN853D_2022), Portuguese Fundação para a Ciência e a Tecnologia - MCTES (CEECIND/00466/2017), and LAQV-REQUIMTE (UIDB/50006/2020, and UIDP/50006/2020). K.V.G. acknowledges the founding of the Mestrelab Research Center (CIM) through the support of the Galician Innovation Agency (GAIN).

Appendix A. Supplementary data

Supplementary data to this article can be found online at https://doi.org/10.1016/j.molliq.2024.125675.

References

[1] A. Chaudhuri, K. Ramesh, D.N. Kumar, D. Dehari, S. Singh, D. Kumar, A. K. Agrawal, Polymeric micelles: A novel drug delivery system for the treatment of breast cancer, J. Drug Deliv. Sci. Technol. 77 (2022) 103886, https://doi.org/10.1016/j.jddst.2022.103886.

[2] J. Kaur, M. Gulati, F. Zacconi, H. Dureja, R. Loebenberg, M.S. Ansari, O. AlOmeir, A. Alam, D.K. Chellappan, G. Gupta, N.K. Jha, T. de J.A. Pinto, A. Morris, Y. E. Choonara, J. Adams, K. Dua, S.K. Singh, Biomedical Applications of polymeric micelles in the treatment of diabetes mellitus: Current success and future approaches, Expert Opin Drug Deliv. 19 (2022) 771–793, https://doi.org/10.1080/17425247.2022.2087629.

[3] J. Kaur, M. Gulati, B. Kapoor, N.K. Jha, P.K. Gupta, G. Gupta, D.K. Chellappan, H. P. Devkota, P. Prasher, M.S. Ansari, F.F. Aba Alkhayl, M.F. Arshad, A. Morris, Y. E. Choonara, J. Adams, K. Dua, S.K. Singh, Advances in designing of polymeric micelles for biomedical application in brain related diseases, Chem. Biol. Interact. 361 (2022) 109960, https://doi.org/10.1016/j.cbi.2022.109960.

[4] D.T. Pham, A. Chokamonsirikun, V. Phattaravorakarn, W. Tiyaboonchai, Polymeric micelles for pulmonary drug delivery: a comprehensive review, J. Mater. Sci. 56 (2021) 2016–2036, https://doi.org/10.1007/s10853-020-05361-4.

[5] M.A. Grimaudo, S. Pescina, C. Padula, P. Santi, A. Concheiro, C. Alvarez-Lorenzo, S. Nicoli, Topical application of polymeric nanomicelles in ophthalmology: a review on research efforts for the noninvasive delivery of ocular therapeutics, Expert Opin. Drug Deliv. 16 (2019) 397–413, https://doi.org/10.1080/17425247.2019.1597848.

[6] S. Kotta, H.M. Aldawsari, S.M. Badr-Eldin, A.B. Nair, K. YT, Progress in Polymeric Micelles for Drug Delivery Applications, Pharmaceutics. 14 (2022) 1636, https://doi.org/10.3390/pharmaceutics14081636.

[7] I. Jarak, M. Pereira-Silva, A.C. Santos, F. Veiga, H. Cabral, A. Figueiras, Multifunctional polymeric micelle-based nucleic acid delivery: Current advances and future perspectives, Appl. Mater. Today. 25 (2021) 101217, https://doi.org/10.1016/j.apmt.2021.101217.

[8] J. Ren, Y. Cao, L. Li, X. Wang, H. Lu, J. Yang, S. Wang, Self-assembled polymeric micelle as a novel mRNA delivery carrier, J. Control. Release. 338 (2021) 537–547, https://doi.org/10.1016/j.jconrel.2021.08.061.

[9] X. Zheng, J. Xie, X. Zhang, W. Sun, H. Zhao, Y. Li, C. Wang, An overview of polymeric nanomicelles in clinical trials and on the market, Chinese Chem. Lett. 32 (2021) 243–257, https://doi.org/10.1016/j.cclet.2020.11.029.

[10] R. Aqeel, N. Srivastava, P. Kushwaha, Micelles in Cancer Therapy: An Update on Preclinical and Clinical Status, Recent Pat. Nanotechnol. 16 (2022) 283–294, https://doi.org/10.2174/1872210515666210720125717.

[11] S. Ghosh, A. Ray, N. Pramanik, Self-assembly of surfactants: An overview on general aspects of amphiphiles, Biophys. Chem. 265 (2020) 106429, https://doi.org/10.1016/j.bpc.2020.106429.

[12] D.V. Bhalani, B. Nutan, A. Kumar, A.K. Singh Chandel, Bioavailability Enhancement Techniques for Poorly Aqueous Soluble Drugs and Therapeutics, Biomedicines. 10 (2022) 2055, https://doi.org/10.3390/biomedicines10092055.

[13] D. Hwang, J.D. Ramsey, A.V. Kabanov, Polymeric micelles for the delivery of poorly soluble drugs: From nanoformulation to clinical approval, Adv. Drug Deliv. Rev. 156 (2020) 80–118, https://doi.org/10.1016/j.addr.2020.09.009.

[14] F. Prencipe, C. Diaferia, F. Rossi, L. Ronga, D. Tesauro, Forward Precision Medicine: Micelles for Active Targeting Driven by Peptides, Molecules 26 (2021) 4049, https://doi.org/10.3390/molecules26134049.

[15] P. Mi, H. Cabral, K. Kataoka, Ligand-Installed Nanocarriers toward Precision Therapy, Adv. Mater. 32 (2020) 1902604, https://doi.org/10.1002/adma.201902604.

[16] Q. Wang, K. Atluri, A.K. Tiwari, R.J. Babu, Exploring the Application of Micellar Drug Delivery Systems in Cancer Nanomedicine, Pharmaceuticals. 16 (2023) 433, https://doi.org/10.3390/ph16030433.

[17] S.K. Hari, A. Gauba, N. Shrivastava, R.M. Tripathi, S.K. Jain, A.K. Pandey, Polymeric micelles and cancer therapy: an ingenious multimodal tumor-targeted drug delivery system, Drug Deliv, Transl. Res. 13 (2023) 135–163, https://doi.org/10.1007/s13346-022-01197-4.

[18] B. Ghosh, S. Biswas, Polymeric micelles in cancer therapy: State of the art, J. Control. Release. 332 (2021) 127–147, https://doi.org/10.1016/j.jconrel.2021.02.016.

[19] R. Bholakant, B. Dong, X. Zhou, X. Huang, C. Zhao, D. Huang, Y. Zhong, H. Qian, W. Chen, J. Feijen, Multi-functional polymeric micelles for chemotherapy-based combined cancer therapy, J. Mater. Chem. B 9 (2021) 8718–8738, https://doi.org/10.1039/D1TB01771C.

[20] N. Avramović, B. Mandić, A. Savić-Radojević, T. Simić, Polymeric Nanocarriers of Drug Delivery Systems in Cancer Therapy, Pharmaceutics. 12 (2020) 298, https://doi.org/10.3390/pharmaceutics12040298.

[21] N. Majumder, N.G. Das, S.K. Das, Polymeric micelles for anticancer drug delivery, Ther. Deliv. 11 (2020) 613–635, https://doi.org/10.4155/tde-2020-0008.

[22] Y.K. Sung, S.W. Kim, Recent advances in polymeric drug delivery systems, Biomater. Res. 24 (2020) 12, https://doi.org/10.1186/s40824-020-00190-7.

[23] A. Bose, D. Roy Burman, B. Sikdar, P. Patra, Nanomicelles: Types, properties and applications in drug delivery, IET Nanobiotechnol. 15 (2021) 19–27, https://doi.org/10.1049/nbt2.12018.

[24] Y. Lu, Z. Yue, J. Xie, W. Wang, H. Zhu, E. Zhang, Z. Cao, Micelles with ultralow critical micelle concentration as carriers for drug delivery, Nat. Biomed. Eng. 2 (2018) 318–325, https://doi.org/10.1038/s41551-018-0234-x.

[25] J. Kaur, V. Mishra, S.K. Singh, M. Gulati, B. Kapoor, D.K. Chellappan, G. Gupta, H. Dureja, K. Anand, K. Dua, G.L. Khatik, K. Gowthamarajan, Harnessing amphiphilic polymeric micelles for diagnostic and therapeutic applications: Breakthroughs and bottlenecks, J. Control. Release. 334 (2021) 64–95, https://doi.org/10.1016/j.jconrel.2021.04.014.
[26] F. Selmin, U.M. Musazzi, G. Magri, P. Rocco, F. Cilurzo, P. Minghetti, Regulatory aspects and quality controls of polymer-based parenteral long-acting drug products: the challenge of approving copies, Drug Discov. Today. 25 (2020) 321–329, https://doi.org/10.1016/j.drudis.2019.12.008.
[27] Y. Herdiana, N. Wathoni, S. Shamsuddin, M. Muchtaridi, Scale-up polymeric-based nanoparticles drug delivery systems: Development and challenges, OpenNano. 7 (2022) 100048, https://doi.org/10.1016/j.onano.2022.100048.
[28] R. Kashapov, G. Gaynanova, D. Gabdrakhmanov, D. Kuznetsov, R. Pavlov, K. Petrov, L. Zakharova, O. Sinyashin, Self-Assembly of Amphiphilic Compounds as a Versatile Tool for Construction of Nanoscale Drug Carriers, Int. J. Mol. Sci. 21 (2020) 6961, https://doi.org/10.3390/ijms21186961.
[29] C. Ceresa, L. Fracchia, A.C. Sansotera, M.A. De Rienzo, I.M. Banat, Harnessing the Potential of Biosurfactants for Biomedical and Pharmaceutical Applications, Pharmaceutics. 15 (2023) 2156, https://doi.org/10.3390/pharmaceutics15082156.
[30] I. Anestopoulos, D.E. Kiousi, A. Klavaris, A. Galanis, K. Salek, S.R. Euston, A. Pappa, M.I. Panayiotidis, Surface Active Agents and Their Health-Promoting Properties: Molecules of Multifunctional Significance, Pharmaceutics. 12 (2020) 688, https://doi.org/10.3390/pharmaceutics12070688.
[31] G. Gaynanova, L. Vasileva, R. Kashapov, D. Kuznetsova, R. Kushnazarova, A. Tyryshkina, E. Vasilieva, K. Petrov, L. Zakharova, O. Sinyashin, Self-Assembling Drug Formulations with Tunable Permeability and Biodegradability, Molecules 26 (2021) 6786, https://doi.org/10.3390/molecules26226786.
[32] A. Figueiras, C. Domingues, I. Jarak, A.I. Santos, A. Parra, A. Pais, C. Alvarez-Lorenzo, A. Concheiro, A. Kabanov, H. Cabral, F. Veiga, New Advances in Biomedical Application of Polymeric Micelles, Pharmaceutics. 14 (2022) 1700, https://doi.org/10.3390/pharmaceutics14081700.
[33] H.M. Aliabadi, A. Lavasanifar, Polymeric micelles for drug delivery, Expert Opin. Drug Deliv. 3 (2006) 139–162, https://doi.org/10.1517/17425247.3.1.139.
[34] N. Wang, X. Cheng, N. Li, H. Wang, H. Chen, Nanocarriers and Their Loading Strategies, Adv. Healthc. Mater. 8 (2019) 1801002, https://doi.org/10.1002/adhm.201801002.
[35] M. Ghezzi, S. Pescina, C. Padula, P. Santi, E. Del Favero, L. Cantù, S. Nicoli, Polymeric micelles in drug delivery: An insight of the techniques for their characterization and assessment in biorelevant conditions, J. Control. Release. 332 (2021) 312–336, https://doi.org/10.1016/j.jconrel.2021.02.031.
[36] X. Zhang, C. Wang, Supramolecular amphiphiles, Chem. Soc. Rev. 40 (2011) 94–101, https://doi.org/10.1039/B919678C.
[37] G. Yu, K. Jie, F. Huang, Supramolecular Amphiphiles Based on Host-Guest Molecular Recognition Motifs, Chem. Rev. 115 (2015) 7240–7303, https://doi.org/10.1021/cr5005315.
[38] H.-W. Tian, Y.-C. Liu, D.-S. Guo, Assembling features of calixarene-based amphiphiles and supra-amphiphiles, Mater. Chem. Front. 4 (2020) 46–98, https://doi.org/10.1039/C9QM00489K.
[39] Y.-C. Pan, X.-Y. Hu, D.-S. Guo, Biomedical Applications of Calixarenes: State of the Art and Perspectives, Angew. Chem. Int. Ed. 60 (2021) 2768–2794, https://doi.org/10.1002/anie.201916380.
[40] A.-N. Lazar, F. Perret, M. Perez-Lloret, M. Michaud, A.W. Coleman, Promises of anionic calix[n]arenes in life science: State of the art in 2023, Eur. J. Med. Chem. 264 (2024) 115994, https://doi.org/10.1016/j.ejmech.2023.115994.
[41] P. Pospíšil, L. Cwiklik, J. Sýkora, M. Hof, G.M. Greetham, M. Towrie, A. Vlček, Solvent-Dependent Excited-State Evolution of Prodan Dyes, J. Phys. Chem. B 125 (2021) 13858–13867, https://doi.org/10.1021/acs.jpcb.1c09030.
[42] M.S. Orellano, D.A. Chiappetta, J.J. Silber, R.D. Falcone, N.M. Correa, Monitoring the microenvironment inside polymeric micelles using the fluorescence probe 6-propionyl-2-dimethylaminonaphthalene (PRODAN), J. Mol. Liq. 343 (2021) 117552, https://doi.org/10.1016/j.molliq.2021.117552.
[43] A. Ali, S. Uzair, N.A. Malik, M. Ali, Study of interaction between cationic surfactants and cresol red dye by electrical conductivity and spectroscopy methods, J. Mol. Liq. 196 (2014) 395–403, https://doi.org/10.1016/j.molliq.2014.04.013.
[44] O.A. Kucherak, P. Didier, Y. Mély, A.S. Klymchenko, Fluorene Analogues of Prodan with Superior Fluorescence Brightness and Solvatochromism, J. Phys. Chem. Lett. 1 (2010) 616–620, https://doi.org/10.1021/jz9003685.
[45] C. Reichardt, Solvatochromic Dyes as Solvent Polarity Indicators, Chem. Rev. 94 (1994) 2319–2358, https://doi.org/10.1021/cr00032a005.
[46] M. Sayed, H. Pal, Supramolecularly assisted modulations in chromophoric properties and their possible applications: an overview, J. Mater. Chem. C 4 (2016) 2685–2706, https://doi.org/10.1039/C5TC03321G.
[47] N. Basilio, B. Gómez, L. Garcia-Rio, V. Francisco, Using Calixarenes To Model Polyelectrolyte Surfactant Nucleation Sites, Chem. Eur. J. 19 (2013) 4570–4576, https://doi.org/10.1002/chem.201203377.
[48] N. Basilio, L. García-Río, Sulfonated Calix[6]arene Host-Guest Complexes Induce Surfactant Self-Assembly, Chem. Eur. J. 15 (2009) 9315–9319, https://doi.org/10.1002/chem.200901065.
[49] V. Wintgens, J.G. Harangozó, Z. Miskolczy, J.-M. Guigner, C. Amiel, L. Biczók, Effect of Headgroup Variation on the Self-Assembly of Cationic Surfactants with Sulfonatocalix[6]arene, Langmuir 33 (2017) 8052–8061, https://doi.org/10.1021/acs.langmuir.7b01941.
[50] J.G. Harangozó, V. Wintgens, Z. Miskolczy, J.-M. Guigner, C. Amiel, L. Biczók, Effect of Macrocycle Size on the Self-Assembly of Methylimidazolium Surfactant with Sulfonatocalix[n]arenes, Langmuir 32 (2016) 10651–10658, https://doi.org/10.1021/acs.langmuir.6b02823.
[51] N. Basílio, D.A. Spudeit, J. Bastos, L. Scorsin, H.D. Fiedler, F. Nome, L. García-Río, Exploring the charged nature of supramolecular micelles based on p-sulfonatocalix[6]arene and dodecyltrimethylammonium bromide, Phys. Chem. Chem. Phys. 17 (2015) 26378–26385, https://doi.org/10.1039/C5CP03718B.
[52] E. Blanco, H. Shen, M. Ferrari, Principles of nanoparticle design for overcoming biological barriers to drug delivery, Nat. Biotechnol. 33 (2015) 941–951, https://doi.org/10.1038/nbt.3330.
[53] H.-W. Tian, Z. Xu, H.-B. Li, X.-Y. Hu, D.-S. Guo, Study on assembling compactness of amphiphilic calixarenes by fluorescence anisotropy, Supramol. Chem. 33 (2021) 527–533, https://doi.org/10.1080/10610278.2022.2087523.
[54] F. Alexis, E. Pridgen, L.K. Molnar, O.C. Farokhzad, Factors Affecting the Clearance and Biodistribution of Polymeric Nanoparticles, Mol. Pharm. 5 (2008) 505–515, https://doi.org/10.1021/mp800051m.
[55] A.E. Nel, L. Mädler, D. Velegol, T. Xia, E.M.V. Hoek, P. Somasundaran, F. Klaessig, V. Castranova, M. Thompson, Understanding biophysicochemical interactions at the nano–bio interface, Nat. Mater. 8 (2009) 543–557, https://doi.org/10.1038/nmat2442.
[56] P. Zhang, D. Chen, L. Li, K. Sun, Charge reversal nano-systems for tumor therapy, J. Nanobiotechnology. 20 (2022) 31, https://doi.org/10.1186/s12951-021-01221-8.
[57] M. Zhang, X. Chen, C. Li, X. Shen, Charge-reversal nanocarriers: An emerging paradigm for smart cancer nanomedicine, J. Control. Release. 319 (2020) 46–62, https://doi.org/10.1016/j.jconrel.2019.12.024.